Journal of the Serbian Chemical Society
JSCS-info@shd.org.rs • www.shd.org.rs/JSCS
J. Serb. Chem. Soc. 76 (4) 557–573 (2011)
JSCS–4142
UDC 536.722:517.544.4:533.912
Original scientific paper

On the relationship between molecular spectroscopy and statistical mechanics: calculation of vibrational–rotational energy levels and partition functions in the ground electronic state of BC_2

MILAN V. SENĆANSKI[1#], LJILJANA STOJANOVIĆ[2], STANKA JEROSIMIĆ[2], JELENA RADIĆ-PERIĆ[2] and MILJENKO PERIĆ[2*#]

[1]*Innovation Centre of the Faculty of Chemistry, University of Belgrade, Studentski Trg 12–16, 11158 Belgrade and* [2]*Faculty of Physical Chemistry, University of Belgrade, Studentski Trg 12–16, P. O. Box 47, 11158 Belgrade, Serbia*

(Received 26 November 2010)

Abstract: The results of extensive *ab initio* calculations of the vibrational–rotational energy spectrum in the ground electronic state of the BC_2 molecule are presented. These data were employed to discuss the evaluation of the corresponding partition functions. Special attention was paid to the problems connected with the calculation of the partition functions for the bending vibrations and rotations about the axis corresponding to the smallest moment of inertia.

Keywords: vibrational–rotational energy; partition functions; BC_2.

INTRODUCTION

In the preceding paper[1] (in further text: Paper I), the evaluation of the partition functions in triatomic molecules undergoing large-amplitude bending vibrations was outlined. In the present paper, the results of *ab initio* calculations of the vibrational–rotational energy levels are reported and the evaluation of the corresponding partition functions for the ground electronic state of the BC_2 molecule is discussed. A major part of the data required for these calculations was generated in a previous study.[2] They were completed in the present work by stretching vibrational frequencies computed at several values of the bending coordinates in order to construct the effective bending potential curves, which were employed in the subsequent handling of large-amplitude bending vibrations and rotations.

* Corresponding author. E-mail: peric@ffh.bg.ac.rs
# Serbian Chemical Society member.
doi: 10.2298/JSC101126053S

In the present study, the Jacobi coordinates *r*, *R* and θ were employed. R is the distance between the C nuclei, r the distance between the B atom and the midpoint of the C–C diatomic and θ is defined as the angle between the vectors $\vec{r}$ and $\vec{R}$ (Fig. 1 of Paper I; in the present case, the *z*-axis lies at the C_{2v} molecular geometry along $\vec{r}$). These coordinates were also used in an extensive *ab initio* study of the rovibrational spectrum in the ground state of BC_2 performed by Leonard *et al.*[3] There is some confusion concerning the assignment of the vibrational modes in BC_2 (see Section 3.1.4 of Ref. 2). Here, the notation consistent with that introduced in Paper I will be used.[1] The stretching modes will be denoted by subscripts *s*1 and *s*2, where *s*1 stands for the higher-frequency mode (predominately C–C) and *s*2 for the lower-frequency one (predominately B–C_2). The name "angular" or "bending" coordinate is used for θ. However, it should be born in mind that this angle is not the bending angle usually used in spectroscopy, namely the angle between the B–C and C–C bonds (or its supplement) – around the equilibrium geometry (roughly of C_{2v} symmetry) the Jacobi coordinate θ in the present case (B and C atoms of similar mass) is even more similar to the antisymmetric stretching than to the bending valence coordinate.

CALCULATION OF THE EFFECTIVE BENDING POTENTIAL CURVES

The potential energy surface (PES) for the ground electronic state of BC_2 was calculated[2] at various levels of sophistication, by means of the MOLPRO *ab initio* software package.[4] In the present study, the data obtained at the RCCSD(T) level of theory, with the cc-pVQZ atomic orbital basis set, were employed. Instead of computing a complete three-dimensional PES by systematically varying all three Jacobi coordinates, as Leonard *et al.*[3] did, attention was concentrated on the angular variable θ, *i.e.*, an effective bending potential curve was computed by optimizing the values of the stretching coordinates *r* and *R* at a number of values of θ. At this level of theory, the global minimum on the PES corresponds to the angle θ = 84.4°, slightly differing from that (90°) of the C_{2v} geometry, at *R*(= C–C) = 1.279 Å, *r*(=B–C2) = 1.379 Å. Thus the ground state is X^2A' (C_s--point group). However, it lies only roughly 20 cm^{-1} below the energy location of the isosceles triangle ($^2A_1$ species of the C_{2v} group). At the linear nuclear arrangement (B–C–C) and C–C and C–B bond lengths of 1.286 and 1.379 Å, respectively (*i.e.*, at *R*(= C–C) = 1.286 Å; *r*(=B–C2) = 2.022 Å), there is a shallow local minimum on the PES; it lies 216 cm^{-1} below the transition state on the minimum energy path towards the global minimum on the PES. This linear species is of $^2\Sigma^+$ symmetry and it is located 2110 cm^{-1} above the global minimum. Leonard *et al.*[3] reported a value of 2204 cm^{-1} for the same quantity. The barrier on the way from the X^2A' to the $^2\Sigma^+$ state was computed to be 2325 cm^{-1} (compared to 2383 cm^{-1} from the literature[3]). At each value of θ where the bond lengths were relaxed, the local harmonic stretching frequencies were calculated

too. All these results are collected in Table I. Graphical presentations of these quantities are shown in Figs. 1–4. It can be noted that the r = B–C2 stretching coordinate and both stretching vibrational frequencies strongly depend on the angular coordinate θ (the variation of the R = C–C stretching coordinate is relatively weak). Therefore, the coupling of the angular and both stretching vibrational modes in the present case is appreciable and cannot be neglected if reliable results for the vibrational energy levels and the corresponding partition functions are be obtained. A consequence of the strong variation of the r = B–C2 distance with θ is an appreciable dependence of the moments of inertia on the angular coordinate. At the equilibrium geometry (X^2A'), the rotational constants are A = = 1.7175, B = 1.1770 and C = 0.6984 cm^{-1}. At the local minimum corresponding to the linear molecular geometry, B = 0.4136 cm^{-1}. These results agree reasonably with those obtained by Leonard *et al.*[3] (A = 1.7224, B= 1.1814, C = 0.6932 cm^{-1} at the global minimum of the PES – indeed, Leonard *et al.* found it to be of C_{2v} symmetry – and B = 0.4232 cm^{-1} at the linear geometry). The same is true for the stretching vibrational frequencies. The present values at the equilibrium geometry of the molecule are $\tilde{\nu}_{s1}$ = 1733 cm^{-1} and $\tilde{\nu}_{s2}$ = 1213 cm^{-1}, while those from the literature[3] are 1678 and 1180 cm^{-1}; the only known experimental result[5] is $\tilde{\nu}$ =1194.6 cm^{-1} for the lower-frequency stretching vibration.

TABLE I. Angular dependence of the electronic energy, internuclear distances and local stretching vibrational frequencies in the ground electronic state of BC2 calculated at the RCCSD(T)/ /cc-pVQZ level of theory

θ / °	R(=C–C) Å	C–B Å	r(=B–C_2) Å	E Hartree	E/hc cm^{-1}	$\tilde{\nu}_{s1}$ cm^{-1}	$\tilde{\nu}_{s2}$ cm^{-1}
0.00	1.2858	1.3792	2.0221	–100.618957	2109	1906	1165
6.82	1.2858	1.3793	2.0156	–100.618864	2130	–	–
13.67	1.2862	1.3797	1.9962	–100.618610	2185	–	–
20.57	1.2867	1.3803	1.9640	–100.618279	2258	–	–
27.55	1.2874	1.3811	1.9193	–100.618006	2318	–	–
34.64	1.2883	1.3821	1.8627	–100.617975	2325	1805	1307
41.88	1.2891	1.3831	1.7944	–100.618399	2232	–	–
49.32	1.2896	1.3844	1.7155	–100.619487	1993	1805	1403
57.04	1.2892	1.3867	1.6275	–100.621407	1571	1748	1440
65.19	1.2875	1.3926	1.5342	–100.624165	966	1705	1439
74.04	1.2844	1.4106	1.4449	–100.627180	304	1700	1353
84.18	1.2793	1.4610	1.3800	–100.628568	0	–	–
84.4044	1.2790	1.4623	1.3789	–100.628569	0	1733	1213
87.04	1.2779	1.4846	1.3734	–100.628544	5	–	–
90.00	1.2771	1.5133	1.3715	–100.628518	11	1746	1200

Adding to the optimized angular potential curve, the stretching vibrational energies $(v_1+1/2)\hbar\omega_{s1} + (v_2+1/2)\hbar\omega_{s2}$, where $\omega_{s1}(\theta)$ and $\omega_{s2}(\theta)$ are the values for the harmonic stretching vibrational frequencies as functions of θ, effective an-

gular potential curves corresponding to the zeroth stretching vibrational level were computed, as well as those for several combinations of the stretching vibrational quantum numbers (v_1 and v_2). Some of them are presented in Fig. 4.

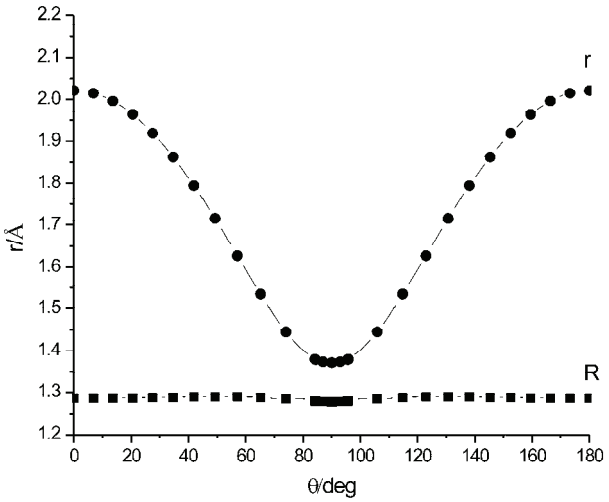

Fig. 1. Dependence of the bond lengths r(=B–C2) and R(C–C) on the bending angle θ in the ground electronic state of BC_2.

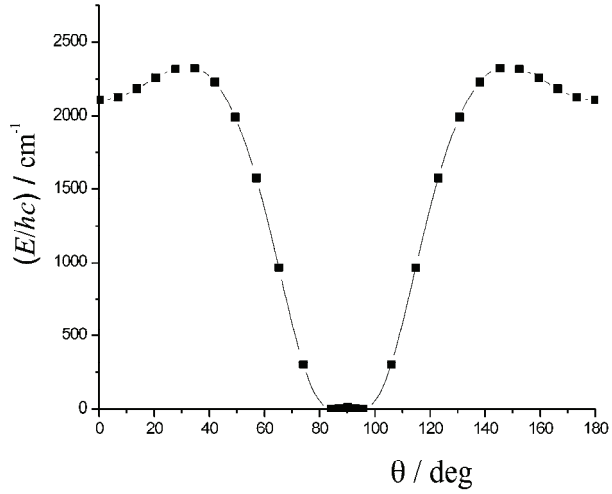

Fig. 2. One-dimensional bending section of the potential energy surface, corresponding to the optimized bond lengths r and R, for the ground electronic state of BC_2.

RESULTS AND DISCUSSION

The energy levels of the Hamiltonian for the angular vibrations and rotations around the z-axis (Eqs. (54)–(56) and (58) from Paper I[1]) were calculated using 100 basis functions, 20 terms in the potential energy expansions, and 15 terms in the expansions of the distances r and R as functions of θ. The results for the l = 0, 1, 2 and 3 quantum numbers are presented in Tables II–VI. Table II comprises the energy levels obtained by employing the minimum-energy angular potential

curve presented in Table I and Fig. 1. The results for four combinations of the stretching quantum numbers (v_{s1} = 0 , v_{s2} = 0; v_{s1} = 0 , v_{s2} = 1; v_{s1} = 1, v_{s2} = 0; v_{s1} = 1 , v_{s2} = 1), obtained by employing the corresponding potentials displayed in Fig. 5, are given in Tables III–VI.

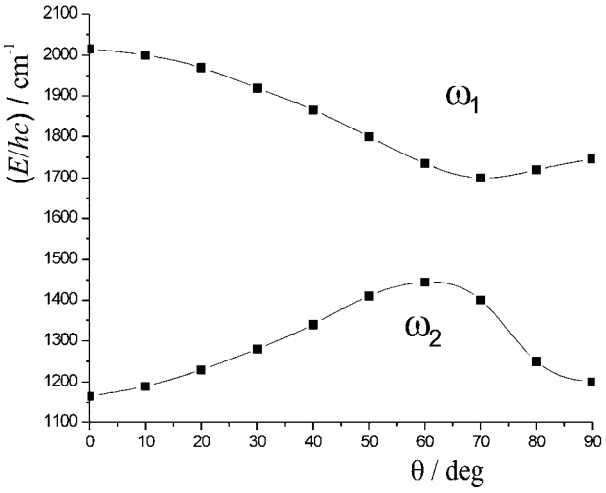

Fig. 3. Dependence of the stretching wave numbers on the bending coordinate θ.

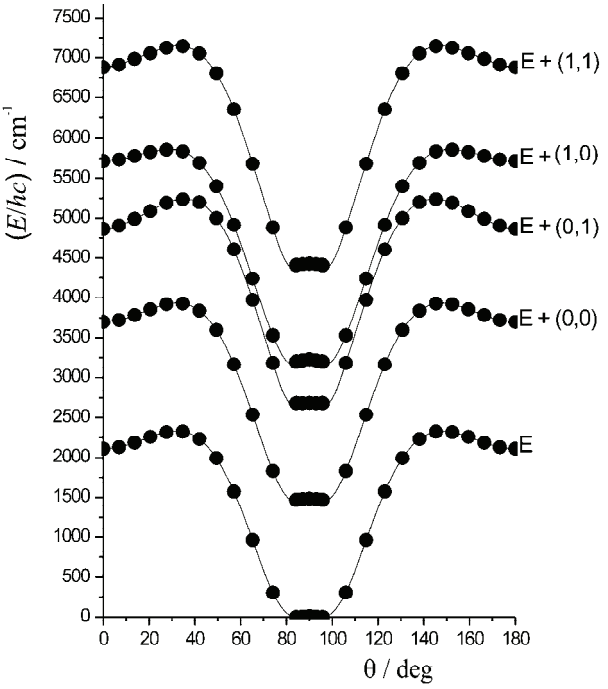

Fig. 4. Effective bending potential curves corresponding to the optimized bond lengths r and R, (E), and the vibrational stretching quantum numbers v_1, v_2, (E + + (v_{s1},v_{s2})).

TABLE II. Bending–*z*-rotational energy levels (in cm^{-1}) calculated using the effective bending potential curve ("minimum") corresponding to the optimized bond lengths. Zero at the energy scale corresponds to the lowest-lying ($v_b = 0$, $l = 0$) vibronic level

Minimum	*l*			
v_b	0	1	2	3
0	0	2	7	16
1	199	200	205	215
2	453	455	461	471
3	710	712	718	728
4	961	963	970	980
5	1200	1202	1209	1220
6	1424	1426	1433	1444
7	1632	1634	1641	1654
8	1821	1824	1832	1845
9	1989	1993	2002	2016
10	2127	2134	2145	2162
11	2130	2216	2252	2276
12	2134	2222	2300	2352
13	2235	2252	2326	2398
14	2282	2323	2382	2453
15	2314	2374	2451	2527
16	2373	2433	2519	2607

TABLE III. Bending–*z*-rotational energy levels calculated using the effective bending potential curve corresponding to the stretching quantum numbers $v_{s1} = 0$, $v_{s2} = 0$. Zero at the energy scale corresponds to the lowest-lying ($v_b = 0$, $l = 0$) vibronic level

(0,0)	*l*			
v_b	0	1	2	3
0	0	2	7	16
1	213	213	218	228
2	481	484	489	499
3	752	754	760	770
4	1015	1017	1023	1034
5	1263	1265	1271	1282
6	1495	1497	1503	1515
7	1710	1712	1720	1732
8	1908	1911	1919	1932
9	2084	2088	2096	2111
10	2234	2237	2247	2264
11	2247	2332	2363	2386
12	2247	2337	2421	2469
13	2347	2360	2445	2517
14	2401	2435	2496	2567
15	2428	2483	2565	2640
16	2484	2538	2630	2721
17	2556	2615	2702	2803
18	2629	2699	2785	2891
19	2708	2786	2877	2986
20	2794	2880	2975	3088

Although it was found that the equilibrium geometry is not exactly C_2v, all energy levels lie above the very small energy barrier (≈ 20 cm^{-1}), so that the molecule behaves effectively as if it had this higher-symmetry configuration. The potential curve has appreciable anharmonicity in the vicinity of the equilibrium geometry as a consequence of the presence of the barrier, which is manifested in the irregular spacing of the vibrational levels – the computed difference between $v_b = 1$ and $v_b = 0$ ($l = 0$) for $v_{s1} = v_{s2} = 0$ (Table III) is much smaller (213 cm^{-1}) than that between $v_b = 2$ and $v_b = 1$ (268), $v_b = 3$ and $v_b = 2$ (271), $v_b = 4$ and $v_b = 3$ (271 cm^{-1}) *etc*. The controversy concerning the question of whether this energy barrier is real will be finally solved when the experimentalists succeed in measuring the energy of the bending fundamental and some of its overtones.

TABLE IV. Bending–*z*-rotational energy levels calculated using the effective bending potential curve corresponding to the stretching quantum numbers $v_{s1} = 0$, $v_{s2} = 1$. Wave number values (in cm^{-1}) are given with respect to the $v_{s1} = 0$, $v_{s2} = 0$, $v_b = 0$, $l = 0$ level

(0,1)	*l*			
v_b	0	1	2	3
0	1224	1225	1231	1239
1	1476	1474	1480	1489
2	1777	1778	1784	1793
3	2077	2080	2086	2096
4	2364	2367	2374	2384
5	2631	2633	2640	2650
6	2876	2876	2883	2894
7	3098	3099	3106	3118
8	3298	3301	3309	3322
9	3437	3478	3487	3502
10	3437	3528	3628	3646
11	3474	3528	3673	3739
12	3614	3618	3679	3770
13	3650	3693	3739	3805
14	3659	3717	3803	3876
15	3727	3762	3852	3952
16	3794	3840	3914	4024
17	3856	3919	3994	4102
18	3927	3999	4082	4190
19	4007	4084	4173	4286
20	4095	4179	4271	4387

Leonard *et al*.[3] performed calculation of all rovibrational states up to the energy of the linear local minimum. We do not find it necessary to compare the present result with theirs; they must differ from one another to some extent because of different handling of the problem (as already mentioned, the approach applied in Ref. 3. was more sophisticated than the present one) and different global-minimum geometry. Instead, the qualitative features of the bending–*z*-ro-

tational spectrum are discussed below, particularly the relationship between the energy-level pattern below and above the potential barrier towards linearity. This topic was not considered in Ref. 3. In the following discussion, the stretching modes are neglected and the results generated employing the minimum-energy angular potential curve are analysed. The results for all vibronic level up to 4000 cm^{-1} are displayed in Fig. 5.

The pattern of the bending plus *z*-rotational levels can be interpreted in an analogous way to the analyses reported in the literature.[6,7] If the bond lengths r and R in the bending–*z*-rotational Hamiltonian, Eqs. (54–56) and (58) of Paper I,[1] are replaced by their equilibrium values r_e and R_e and the following transformation is performed:

$$\begin{aligned} T_3 &= \frac{1}{I_{zz}} = \frac{2}{\mu_r r^2 + \mu_R R^2 - \sqrt{\mu_r^2 r^4 + \mu_R^2 R^4 + 2\mu_r \mu_R r^2 R^2 \cos(2\theta)}} = \\ &= \frac{1}{\sin^2\theta}\left(\frac{1}{\mu_r r^2} + \frac{1}{\mu_R R^2}\right) - \\ &- \frac{2}{\mu_r r^2 + \mu_R R^2 + \sqrt{\mu_r^2 r^4 + \mu_R^2 R^4 + 2\mu_r \mu_R r^2 R^2 \cos(2\theta)}} = \\ &= \frac{1}{\sin^2\theta}\left(\frac{1}{\mu_r r^2} + \frac{1}{\mu_R R^2}\right) - \frac{1}{I_{yy}} \end{aligned} \tag{1}$$

one obtains:

$$\hat{H}_{b,z} = -\frac{\hbar^2}{2\mu_b}\left(\frac{\partial^2}{\partial\theta^2} + \cot\theta\frac{\partial}{\partial\theta} - \frac{l^2}{\sin^2\theta}\right) - Bhcl^2 + V_{r,R}(\theta) \tag{2}$$

with:

$$\frac{1}{\mu_b} = \left(\frac{1}{\mu_r r_e^2} + \frac{1}{\mu_R R_e^2}\right),\ B = \frac{\hbar^2}{2hcI_{yy}} \tag{3}$$

TABLE V. Bending–*z*-rotational energy levels calculated using the effective bending potential curve corresponding to the stretching quantum numbers $v_{s1} = 1$, $v_{s2} = 0$. Wave number values (in cm^{-1}) are given with respect to the $v_{s1} = 0$, $v_{s2} = 0$, $v_b = 0$, $l = 0$ level

(1,0)	*l*			
v_b	0	1	2	3
0	1735	1736	1741	1750
1	1933	1932	1938	1947
2	2198	2200	2206	2216
3	2465	2468	2474	2484
4	2728	2731	2737	2747
5	2979	2981	2987	2998
6	3217	3218	3224	3236
7	3440	3442	3449	3461

TABLE V. Continued

(1,0)	*l*			
v_b	0	1	2	3
8	3648	3651	3659	3672
9	3840	3844	3852	3866
10	4010	4014	4023	4038
11	4155	4157	4168	4186
12	4243	4270	4286	4309
13	4246	4314	4365	4403
14	4272	4327	4406	4466
15	4346	4380	4456	4524
16	4390	4440	4527	4602
17	4443	4498	4597	4688
18	4516	4576	4671	4776
19	4595	4665	4757	4867
20	4678	4757	4852	4966

In this approximation, the kinetic energy operator consists of two terms: the first one is the kinetic energy operator of an isotropic two-dimensional oscillator (when the volume element is: $dV = \sin\theta d\theta d\varphi$) but, at the same time, it represents the complete Hamiltonian of a rigid two-dimensional rotator;[8] the second term can be interpreted as the *l*-dependent correction to it. $V_{r,R}(\theta)$ is the potential for bending vibrations or, alternatively, the potential barrier hindering free rotations of the B-atom around the C–C fragment.

TABLE VI. Bending–*z*-rotational energy levels calculated using the effective bending potential curve corresponding to the stretching quantum numbers $v_{s1} = 1$, $v_{s2} = 1$. Wave number values (in cm^{-1}) are given with respect to the $v_{s1} = 0$, $v_{s2} = 0$, $v_b = 0$, $l = 0$ level

(1,1)	*l*			
v_b	0	1	2	3
0	2960	2961	2966	2975
1	3198	3196	3201	3210
2	3494	3495	3501	3511
3	3791	3794	3800	3810
4	4078	4081	4087	4097
5	4346	4348	4354	4365
6	4595	4595	4602	4614
7	4825	4826	4833	4845
8	5037	5040	5048	5061
9	5230	5234	5242	5256
10	5397	5400	5409	5425
11	5439	5516	5542	5561
12	5439	5518	5622	5661
13	5528	5534	5646	5716
14	5599	5621	5682	5758
15	5622	5666	5753	5827

TABLE VI. Continued

(1,1)	*l*			
v_b	0	1	2	3
16	5667	5711	5813	5910
17	5741	5788	5875	5990
18	5814	5875	5956	6072
19	5890	5962	6047	6163
20	5973	6052	6143	6262

Below the energy corresponding to the linear BCC, particularly around the global minimum of the potential surface, the molecule behaves as a bent one; it is then convenient to write the bending part of the Hamiltonian, Eq. (2), in a form analogous to Eq. (40) of Paper I:[1]

$$\hat{H}_{b,z} = -\frac{\hbar^2}{2\mu_b}\frac{\partial^2}{\partial\theta^2} + Ahcl^2 + V_{r,R}(\theta) \quad (4)$$

where:

$$A = \frac{\hbar^2}{2hcI_{zz}} \quad (5)$$

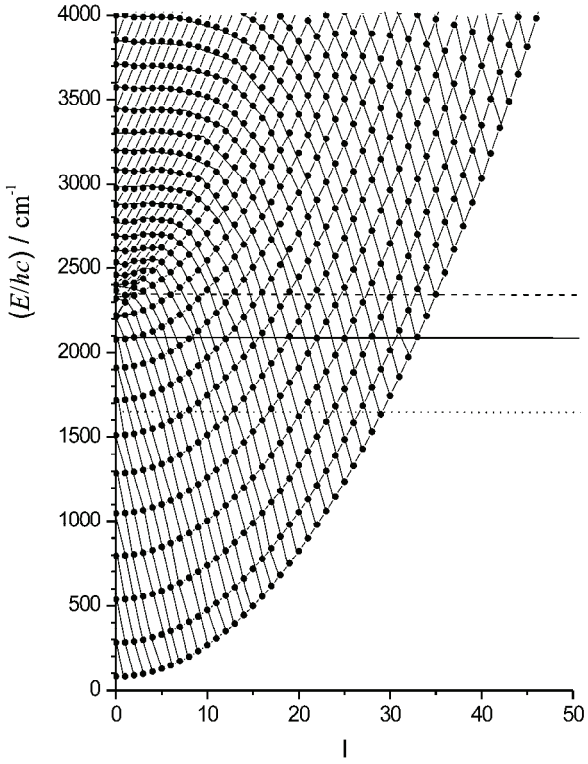

Fig. 5. Bending–*z*-rotational energy levels in the ground electronic state of BC_2. Zero at the energy scale corresponds to the position of the lowest-lying $v_b = 0$, $l = 0$ vibronic level. Full horizontal line: energy position of the local minimum at linear geometry. Dash horizontal line: energy position of the maximum at the barrier between the global and local minimum. Dotted horizontal line: zero energy of the hypothetical free rotator.

This Hamiltonian is obtained from Eq. (2) by replacing the volume element $dV = \sin\theta d\theta d\varphi$ by $dV = d\theta d\varphi$, and absorbing the term (appearing in the transformed kinetic energy operator) $\propto 1/\theta^2 \cong 1/\theta_e^2$ in $V_{r,R}(\theta)$. The first and the third term represent together the Hamiltonian for one-dimensional bending vibrations and the second one, the eigenvalues of the Hamiltonian for rotations about the *z*-axis. In the harmonic approximation, the eigenvalues of the Hamiltonian, Eq. (4), are given by Eq. (41) of Paper I (they are now written without the constant term $\hbar\omega_b/2$):[1]

$$E_{b,z} = \hbar\omega_b v_b + Ahcl^2 \tag{6}$$

Each bending vibrational level is thus accompanied by rotational levels corresponding to $l = 0,1,2,\ldots$, the energies of which depend quadratically on *l*. The $l = 0$ levels are non-degenerated, while the $l \neq 0$ levels are twofold degenerated. The complete approximate bending–rotational energy spectrum can be obtained by adding to these levels the approximate contribution of the *x*,*y* rotations:

$$E^r_{x,y} = \frac{\hbar^2}{2\sqrt{I_{xx}I_{yy}}}\left[J(J+1) - l^2\right] \tag{7}$$

with $J \geq l$. As mentioned in Paper I,[1] if more accurate results are required, we can exclude the second term from the Hamiltonian, Eq. (4), can be excluded and the energy levels of the asymmetric top calculated separately using the properly averaged rotational constants.

Sufficiently far above the potential barrier towards the linear local minimum, there is no potential hindering bending and the Hamiltonian, Eq. (2), effectively reduces to:

$$\hat{H}_{b,z} = -\frac{\hbar^2}{2\mu_b}\left(\frac{\partial^2}{\partial\theta^2} + \cot\theta\frac{\partial}{\partial\theta} - \frac{l^2}{\sin^2\theta}\right) - Bhcl^2 = \frac{1}{2\mu_b}\hat{j}^2 - \frac{l^2\hbar^2}{2I_{yy}} \tag{8}$$

The operator $\hat{j}$ has the same form as the total angular momentum of a linear molecule; a capital (*J*) is not used in order to distinguish this quantity from the total angular momentum involving also *x*- and *y*-rotations. In the harmonic approximation, the eigenvalues of the Hamiltonian, Eq. (8), are:

$$E_{b,z} = E_0 + ahcj(j+1) - Bhcl^2 \tag{9}$$

where E_0 is some reference energy (see below) and:

$$a \equiv \frac{\hbar^2}{2hc\mu_b} = A + B \tag{10}$$

for a given j, the number l takes the values $j, j-1,\ldots,0$. However, the presence of the bending potential reaching a maximum at roughly 2300 cm^{-1} obs-

cures this simple picture. Furthermore, the rotation "constants" cannot be assumed to be constant during large-amplitude motions over all values of θ. For this reason, the values for E_0 (zero point energy of the hypothetical completely free, *i.e.*, without any potential, rotator), a and B in Eq. (9) cannot be derived directly from the *ab initio* computed structural parameters. Instead, one can use, *e.g.*, the computed high-lying $l = 0$ vibronic levels and fit them to Formula (9). In this way, $E_0 = 1634$ cm^{-1}(hc), and $a = 2.51$ cm^{-1} are obtained. Note that this value for a is between those corresponding to the linear geometry ($a_l = 2.245$ cm^{-1}) and the equilibrium (bent) molecular geometry ($a_b = 2.894$ cm^{-1}). The same is true for the effective value for B, which is found to lie between the linear and C_{2v} values of 0.4136 and 1.1770 cm^{-1}, respectively. At small l-values, the values of $j–l$ practically coincide with v_b, the last quantum number playing, in this energy range, solely the role of a running index.

Inspecting the form of the vibronic wave functions, it was found that only the nearly degenerate $l = 0$ levels with $v_b = 10$ and 11 and the $l = 1$ levels with $v_b = 11$ and 12 (Table II and Fig. 5) belong to the local minimum at the linear molecular geometry. The energy difference between the pairs of these $l = 1$ and $l = 0$ levels of roughly 90 cm^{-1}, thus corresponding approximately to the bending frequency of the linear structure. All other vibronic levels belong either to the bent structure with the global minimum close to the C_{2v} geometry (*e.g.*, the v_b from 0 to 9 and 12 levels for $l = 0$, and v_b from 0 to 10 for $l = 1$), or lie above the barrier towards the linearity (among $l = 0$ and $l = 1$ levels, those with $v_b \geq 13$).

The vibronic energy levels below the barrier to linearity (*i.e.*, in the energy region between 0 and roughly 2000 cm^{-1} fit reasonably the energy Formula (6). The lines in Fig. 5 connecting the levels with the same quantum number v_b increase quadratically with increasing l. Small discrepancies are caused by the anharmonicity of the potential, particularly by the presence of the energy hump at the C_{2v} geometry. In Fig. 5, also connected with one another are the energy levels having the same value for $v_b + l \equiv j$ (note that in this energy region, the number j is without any obvious physical meaning, *i.e.*, it is not connected with any real rotational motion). Replacing in Eq. (6) v_b by $j – l$, one obtains:

$$E_{b,z} = \hbar\omega_b j - \hbar\omega_b l + Ahcl^2 \tag{11}$$

For a given j and at a not very large l, the energy given by Eq. (11) linearly decreases with increasing l.

Above the barrier to linearity, the levels with the same "rotational" quantum number j are connected by the lines, which decrease with increasing l. Lines connecting the levels with the same value $j – l = v_b$ with one another are also drawn. According to Eq. (8), they should satisfy the equation:

$$E_{b,z} = E_0 + ahcv_b\left(v_b + 1\right) + ahc\left(2v_b + 1\right)l + Ahcl^2 \tag{12}$$

where again $a = A + B$. At large values of v_b and small l, as in the upper left part of Fig. 5, the energy increases linearly with l. For small values of v_b compared to l, the energy increases quadratically with increasing l in the same manner as the energy of the levels below the barrier with the same quantum number v_b (Eq. (6)). On the other hand, the decreasing curves connecting the levels with the same (high) j value gradually change their second derivative (with respect to l) from $\propto -B$ (Eq. (9)) to $\propto A$ (Eq. (11)) with increasing l.

The complete vibronic energy pattern presented in Fig. 5 is, of course, a combination of both extreme cases discussed above. It gains additional complexity by the presence of the local minimum at the linear geometry and the energy hump at the C_{2v} configuration. Thus, the question is whether partition functions can be reliable computed within the framework of usual approximations such as the harmonic one and that based on the separate handling of the bending vibrations and the z-axis rotations.

The actually computed effective bending potential curve (with a small hump at the C_{2v} geometry), corresponding to the optimized bond lengths and the $l = 0$ and $l = 1$ vibronic levels up to 4000 cm^{-1}, is displayed in Fig. 6. In the same figure, the two lowest-lying $l = 0$ levels computed by using the potential curve

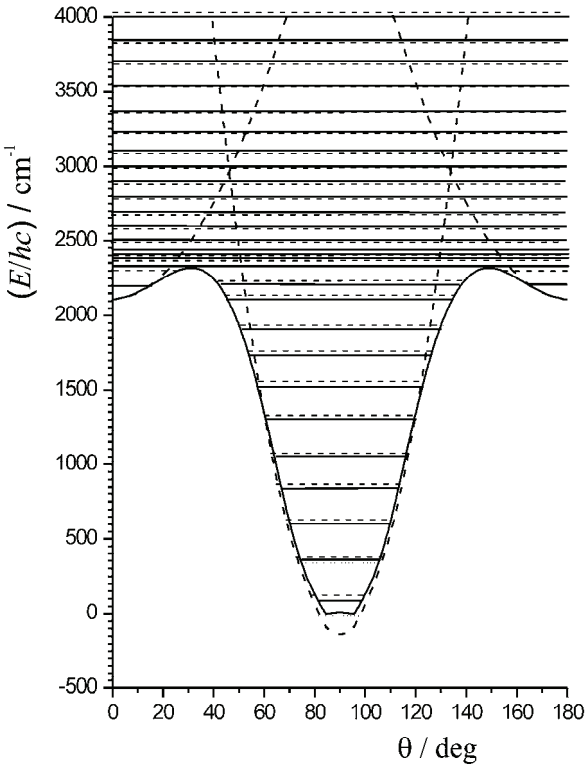

Fig. 6. $l = 0$ (solid horizontal lines) and $l = 1$ (dashed lines) vibronic levels in the ground electronic state of BC_2, calculated employing the effective bending potential curve (with a small hump at the C_{2v} geometry) corresponding to the optimized bond lengths. Dotted horizontal lines denote the two lowest-lying $l = 0$ levels computed using the potential curve having a global minimum at C_{2v} geometry (dotted curve). Dashed potential curves indicate the harmonic approximation of the separate bending potentials for bent and linear equilibrium geometry.

having a global minimum at C_{2v} geometry (as found in some of the previous studies) are presented. Also in Fig. 6, separate harmonic bending potentials having minima at C_{2v} and linear molecular geometry, and the corresponding $l = 0$ and $l = 1$ vibronic levels are shown. In the present case, the partition functions involving bending and *z*-rotational energy levels may be computed at three levels of sophistication: *i*) taking into account only the harmonic potential curve with the minimum at C_{2v} geometry – in this case, the energy is given by Eq. (6), where $\tilde{\nu}_b = 275$ cm^{-1} and the partition function is presented by Eq. (42) of Paper I;[1] *ii*) summing the partition function from the preceding case with that corresponding to the linear two-dimensional harmonic oscillator with the frequency of $\tilde{\nu}_b = 110$ cm^{-1} and the lowest lying vibronic level at $E_0 / hc = 2219$ cm^{-1} above the lowest-lying level of the bent structure – the energy levels of the linear oscillator are given by Eq. (7) of Paper I (without $\hbar\omega_b$ and with the additional E_0), and the corresponding partition function is obtained by multiplying Eq. (14) of Paper I by exp ($-E_0/kT$);[1] *iii*) numerically calculating the partition functions using vibronic levels such as those presented in Fig. 5.

Now, the results obtained by three the procedures described above for two characteristic temperatures, $T = 1000$ K and $T = 5000$ K, are compared with one another. To save time, only partition functions involving energy levels up to 4000 cm^{-1} were computed. This does not ensure full convergence of the results, particularly not for $T = 5000$ K, but gives sufficient information to draw reliable conclusions. Thus, instead of using the analytic formulae for the partition functions in the harmonic approximation, their parts corresponding to the chosen energy region were calculated manually. The double degeneracy of the $l \neq 0$ levels is taken into account and the spin degeneracy (representing a simple multiplicative factor) is ignored. The number of vibronic (bending plus *z*-rotational) energy levels lying in the energy intervals of 100 and 500 cm^{-1} is shown in Fig. 7. It can be seen that the harmonic approximations work reasonably well below the barrier towards the linearity, but they (particularly the first one, in which the presence of the linear structure is ignored) significantly underestimate the number of "rotational" levels above the barrier. Employing the latter set of results (wave number intervals of 500 cm^{-1}), the partition functions were estimated as:

$$Z_{b,z} \cong \sum_{n=1}^{8} N(n) \mathrm{e}^{-\frac{(n-1/2)500\ \mathrm{cm}^{-1} hc}{kT}} \tag{13}$$

where $N(n)$ is the number of levels in the n-th energy interval. At $T = 1000$ K, the partition functions: *i*) 106.5; *ii*) 108.0; *iii*) 118.0 are obtained. The first two numbers are practically identical to those which are obtained by means of the Formulae (42) and (14) of Paper I. The corresponding values at $T = 5000$ K are: *i*) 524.2; *ii*) 582.9; *iii*) 638.4. (Because the energy region between 0 and 4000 cm^{-1} does not ensure convergence of the partition functions at this high temperature,

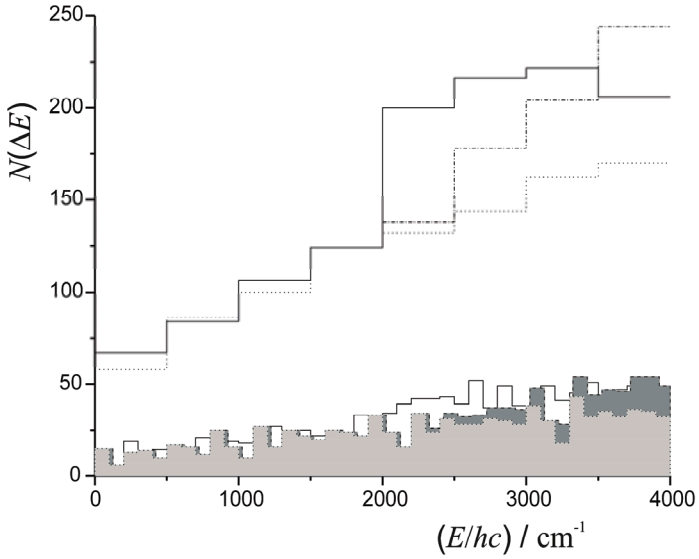

Fig. 7. Numbers of vibronic (bending plus *z*-rotational) energy levels in the ground electronic state of BC_2, lying in the wave number intervals of 100 (bottom) and 500 (top) cm^{-1}. Dotted lines (bright grey in the lower diagram): results obtained with the harmonic approximation only involving C_{2v} configuration. Dash–dotted lines (dark grey in the lower diagram): harmonic approximation, both C_{2v} and linear configurations taken into account. Full lines: results of the variational solution of the Schrödinger equation.

the first two numbers differ considerably from the values obtained employing the analytical Expressions (42) and (14) from Paper I, 1046 and 1592, respectively).

The above analysis leads to the following conclusions. The energy hump at the C_{2v} configuration is too small to cause dramatic irregularities in the bending energy pattern around the equilibrium molecular geometry and, consequently, its presence does not significantly affect the partition functions. On the other hand, the role of the shallow local minimum at linear geometry is completely different in the low- and high-temperature regions. At relatively low temperatures (*e.g.*, at T = 1000 K), the presence of this local minimum, lying about 2000 cm^{-1} above the global minimum, can safely be ignored, because the factor exp ($-E/kT$) strongly quenches its contributions to the partition functions. However, it cannot be ignored if accurate high-temperature partition functions are required. This cannot be clearly seen based on the numbers presented above for T = 5000 K, but becomes quite obvious on comparing Figs. 6 and 8 and inspecting the upper part of Fig. 7. It can be seen that the harmonic approximation in the variant *i* (the presence of the linear structure is ignored) significantly underestimates the number of "rotational" levels above the barrier. On the other hand, approach *ii* tends to overestimate the number of levels in the high-energy region (particularly at T > > 5000 K). Thus, only an approach which takes into account the gradual change

of the structure of the vibrational–rotational spectrum at large-amplitude bending vibrations, such as *iii*, can ensure reliable results in the high-temperature region.

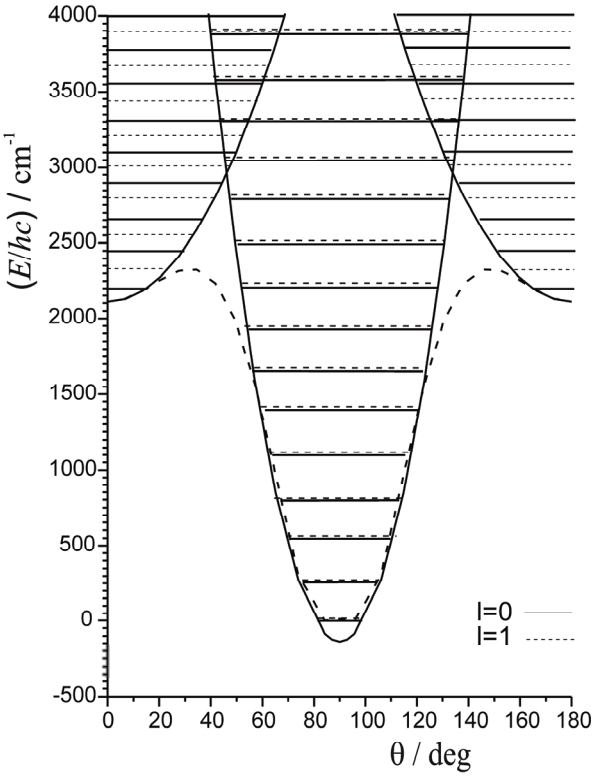

Fig. 8. l = 0 (full horizontal lines) and l = 1 (dashed lines) vibronic levels obtained by replacing the actually computed bending potential (dashed curve) by the harmonic potentials having minima at C_{2v} and linear molecular geometry (solid curves).

It should be stressed once more that the above analysis concerns only the bending–*z*-rotational part of the total partition function. An even more critical point is the evaluation of the contributions of the *x*,*y* rotations. The problems are caused by the much smaller values of the corresponding rotational constants around the linear molecular geometry than in the region close to the global minimum on the potential surface. This part of the partition function cannot be reliably evaluated in harmonic approximations, even at relatively low temperatures.

CONCLUSIONS

In the present paper, the results of extensive *ab initio* calculations of the vibrational–rotational energy spectrum in the ground electronic state of the BC_2 molecule are reported. The corresponding potential energy surface is characterized by a global minimum at slightly distorted C_{2v} geometry, and a local minimum at the linear nuclear arrangement, lying about 2100 cm^{-1} above the global minimum. The potential barrier between these two structures is calculated to be

roughly 2300 cm^{-1}. These facts, as well as the strong stretch–bend coupling cause the vibrational–rotational spectrum to have a rather complex structure. Estimations of the corresponding partition functions, particularly the bending–*z*-rotational one, are discussed in detail.

Acknowledgements. We acknowledge financial support by the Ministry of Science and Technological Development of the Republic of Serbia (Contract Nos. 142074 and 142055).

И З В О Д

ВЕЗА ИЗМЕЂУ МОЛЕКУЛСКЕ СПЕКТРОСКОПИЈЕ И СТАТИСТИЧКЕ МЕХАНИКЕ: РАЧУНАЊЕ ВИБРАЦИОНО–РОТАЦИОНИХ ЕНЕРГИЈСКИХ НИВОА И ПАРТИЦИОНИХ ФУНКЦИЈА У ОСНОВНОМ ЕЛЕКТРОНСКОМ СТАЊУ МОЛЕКУЛА BC_2

МИЛАН В. СЕНЋАНСКИ[1], ЉИЉАНА СТОЈАНОВИЋ[2], СТАНКА ЈЕРОСИМИЋ[2], ЈЕЛЕНА РАДИЋ-ПЕРИЋ[2] и МИЉЕНКО ПЕРИЋ[2]

[1]*Иновациони центар Хемијског факултета Универзитета у Београду и* [2]*Факултет за физичку хемију Универзитета у Београду*

Приказани су резултати опсежних *ab initio* рачунања вибрационо–ротационог енергијског спектра у основном електронском стању молекула BC_2. Ови подаци коришћени су у дискусији о одређивању одговарајућих партиционих функција. Посебна пажња посвећена је проблемима везаним за рачунање партиционих функција за савијајуће вибрације и ротације око осе која кореспондира најмањем моменту инерције.

(Примљено 26. новембра 2010)

REFERENCES

1. M. V. Senćanski, J. Radić-Perić, M. Perić, *J. Serb. Chem. Soc*. **76** (2011) 539
2. S. V. Jerosimić, M. V. Senćanski, J. Radić-Perić, *J. Mol. Struct. Theochem.* **944** (2010) 53
3. C. Leonard, G. Chambaud, P. Rosmus, S. Carter, N. C. Handy, M. Wyss, J. P. Maier, *J. Chem. Phys*. **113** (2000) 5228
4. *MOLPRO, version 2006.1, a package of* ab initio *programs*, http://www.molpro.net
5. J. M. L. Martin, P. R. Taylor, J. P. Yustein, T. R. Burkholder, L. Andrews, *J. Chem. Phys.* **99** (1996) 4927.
6. M. Perić, M. Mladenović, S. D. Peyerimhoff, R. J. Buenker, *Chem. Phys*. **82** (1983) 317
7. M. Perić, M. Mladenović, S. D. Peyerimhoff, R. J. Buenker, *Chem. Phys*. **86** (1984) 85
8. P. R. Bunker, *Molecular Symmetry and Spectroscopy*, Academic Press, New York, 1979.